New Journal of Chemistry

Support Information for:

One-pot synthesis of a recyclable ratiometric fluorescent probe based on MOFs for turn-on sensing of Mg^{2+} ions and bioimaging in live cells

Xuechuan Gao, Yuanyuan Gao, Ruilong Qi, Limin Han*

College of Chemical Engineering, Inner Mongolia University of Technology, Hohhot 010051, PR China

Content

Figure S13 Plot of the observed k versus the concentration of Mg^{2+} ions for the pseudo first-order reaction of Fe_3O_4/RhB@Al-MOFs with varying concentration of Mg^{2+}

Figure S14 Fluorescence measurements of Fe_3O_4/RhB@Al-MOFs after treatment with different pH

Figure S15 XRD patterns of as-synthesized Fe_3O_4/RhB@Al-MOFs (A), Fe_3O_4/RhB@Al-MOFs after detection of Mg^{2+} for five cycles (B) and Fe_3O_4/RhB@Al-MOFs after storaging in water for 7 days (C)

Table 1 Comparison table for various probes for the detection of Mg^{2+} ions.

Figure S16 C1s and O1s XPS for Fe_3O_4/RhB@Al-MOFs and Mg^{2+} treatment of Fe_3O_4/RhB@Al-MOFs

Figure S17 Comparison of the luminescence intensity of Fe_3O_4/RhB@Al-MOFs (I_{440}/I_{610}) in 10^{-3} M solutions of different biologically relevant substances

Figure S18 Fluorescence imaging of live A375 cells after being incubated with Fe_3O_4/RhB@Al-MOFs composite material (A); Fluorescence imaging of live A375 cells after being incubated with Fe_3O_4/RhB@Al-MOFs and Mg^{2+} ions (B).

Figure S19 Viabilities of HL-7702 cells and A373 cells in the presence of Fe_3O_4/RhB@Al-MOFs composite asassayed by MTT.

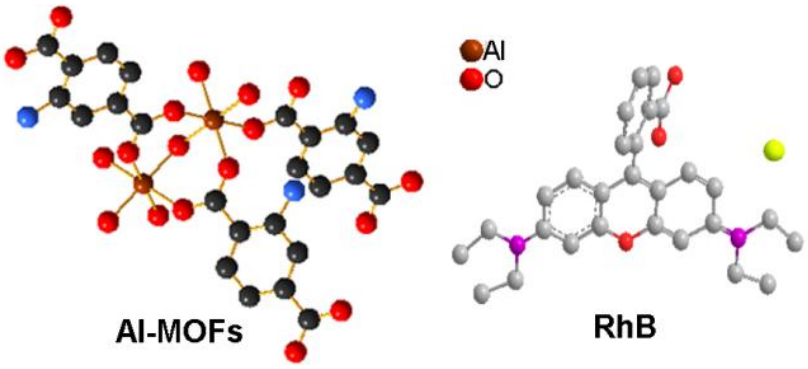

Figure S1 The structure of Al-MOFs and RhB

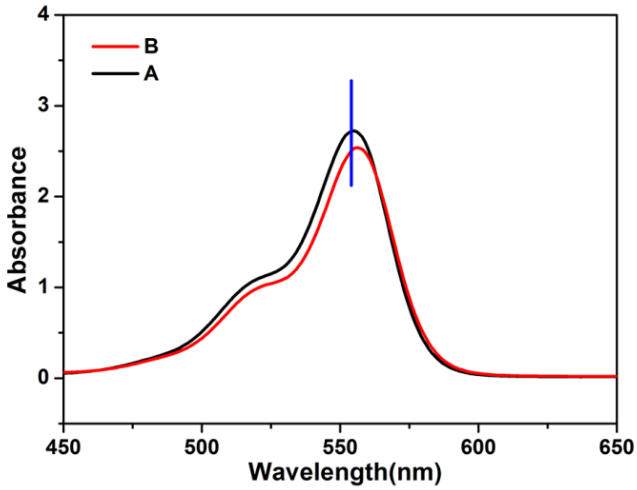

Figure S2 UV-vis absorption spectra of RhB (A) and RhB after interacting with Al^{3+} ions (B).

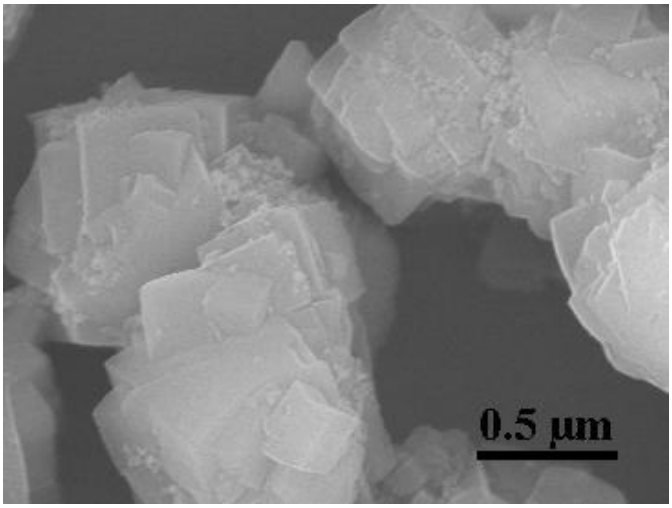

Figure S3 The enlarged SEM images of Fe_3O_4/RhB@Al-MOFs

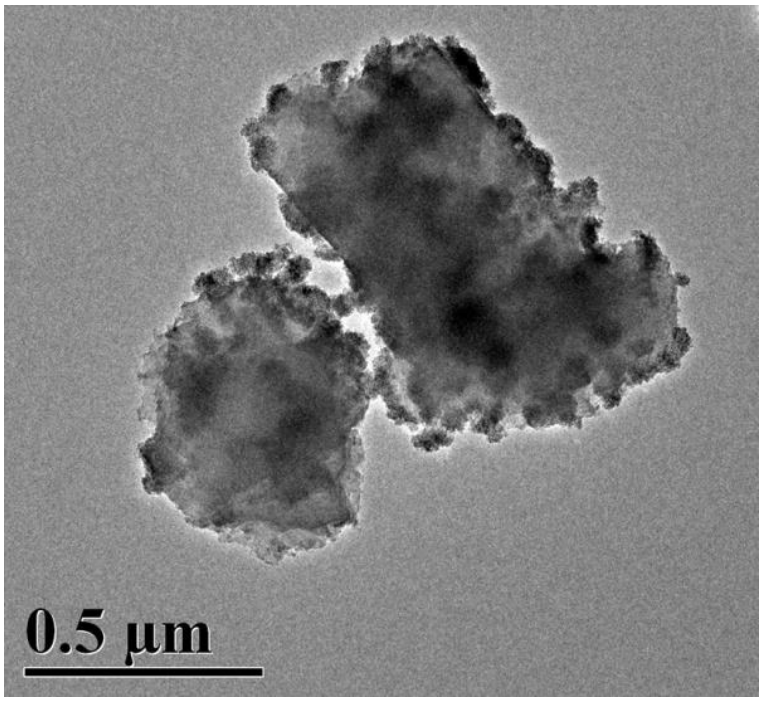

Figure S4 The TEM images of Fe_3O_4/RhB@Al-MOFs

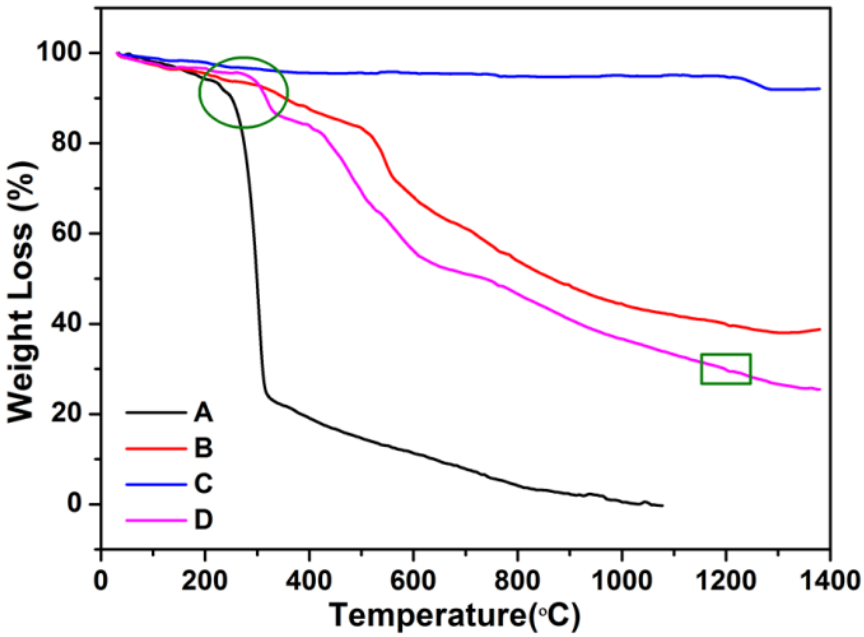

Figure S5 The TGA cures of RhB (A) and Al-MOFs (B), Fe_3O_4 (C) and Fe_3O_4/RhB@Al-MOFs (D)

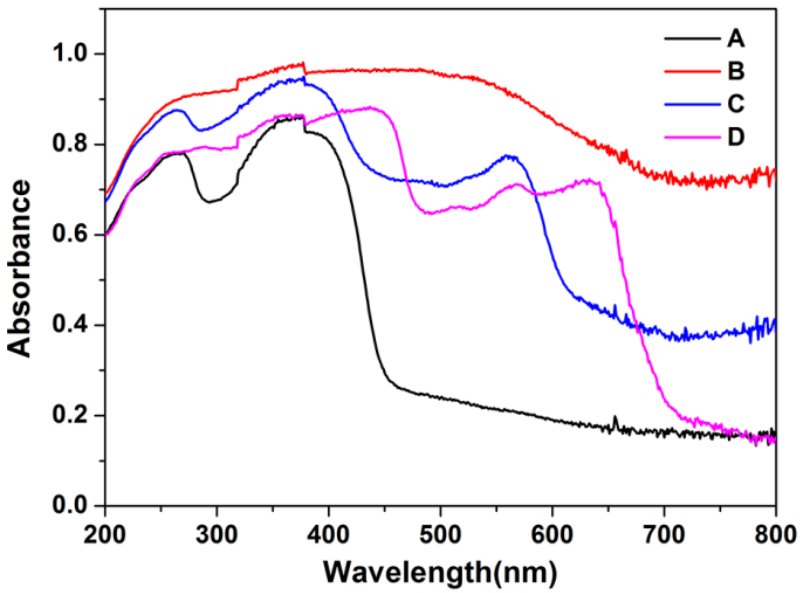

Figure S6 The solid-state UV−vis absorption spectra of Al-MOFs (A), Fe_3O_4 (B) Fe_3O_4/RhB@Al-MOFs (C) and RhB (D)

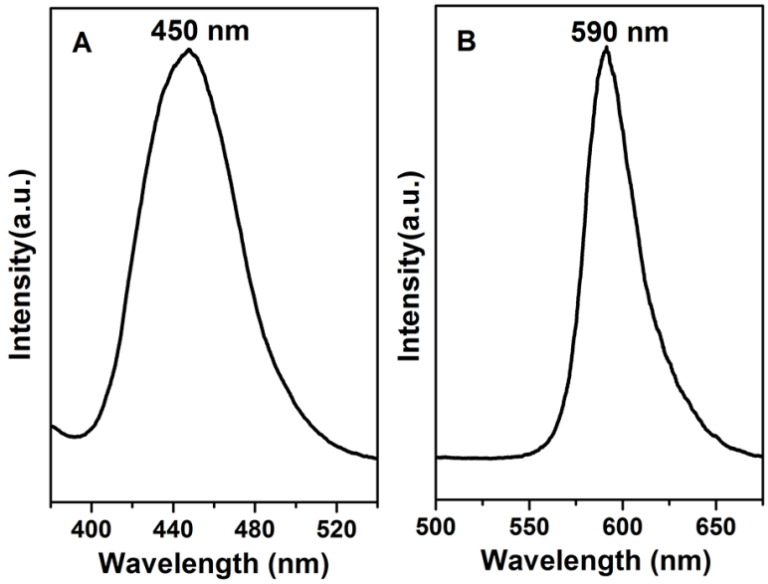

Figure S7 The emission spectra of Al-MOFs (A) and RhB (B) excited at 320 nm

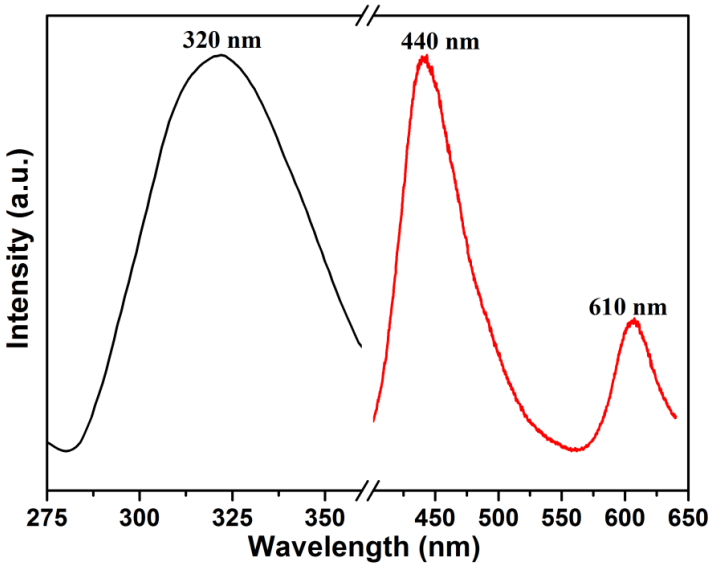

Figure S8 The excitation and emission spectra of Fe_3O_4/RhB@Al-MOFs

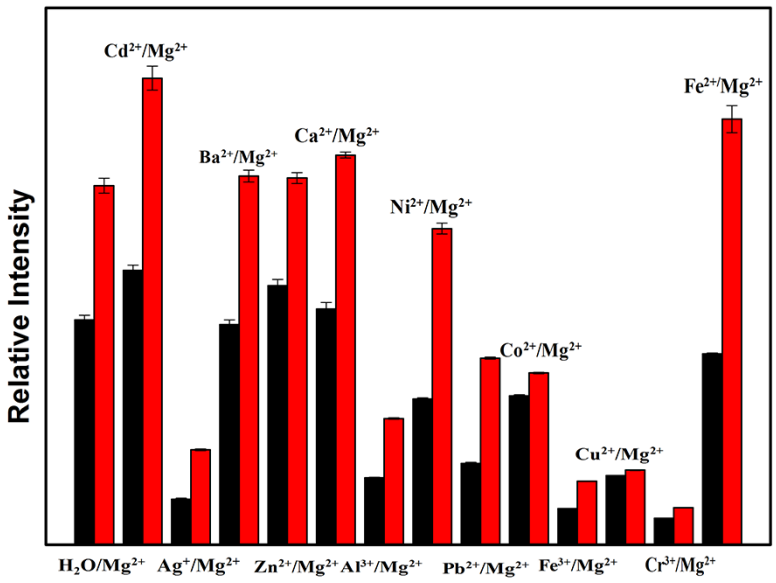

Figure S9 Fluorescence responses of Fe_3O_4/RhB@Al-MOFs (I_{440}/I_{610}) to Mg^{2+} ions among various ions. The blue bars represent the emission intensities of Fe_3O_4/RhB@Al-MOFs (I_{440}/I_{610}) in the presence of 1 $\times 10^{-3}$ M other metal ions. The red bars represent the change of the emission intensities of Fe_3O_4/RhB@Al-MOFs (I_{440}/I_{610}) upon the subsequent addition of 1 $\times 10^{-3}$ M Mg^{2+} ions to the above solution.

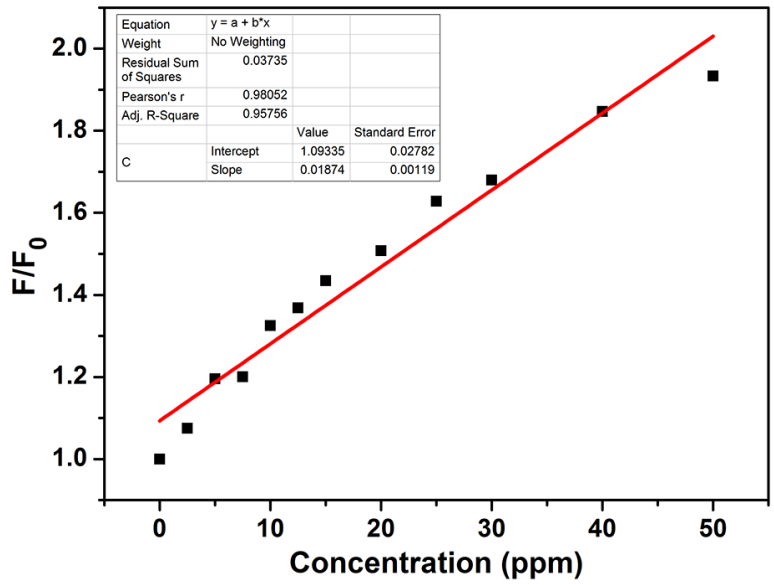

Figure S10 Linear relationship between the fluorescence intensity of Al-MOFs and Mg^{2+} ions concentration

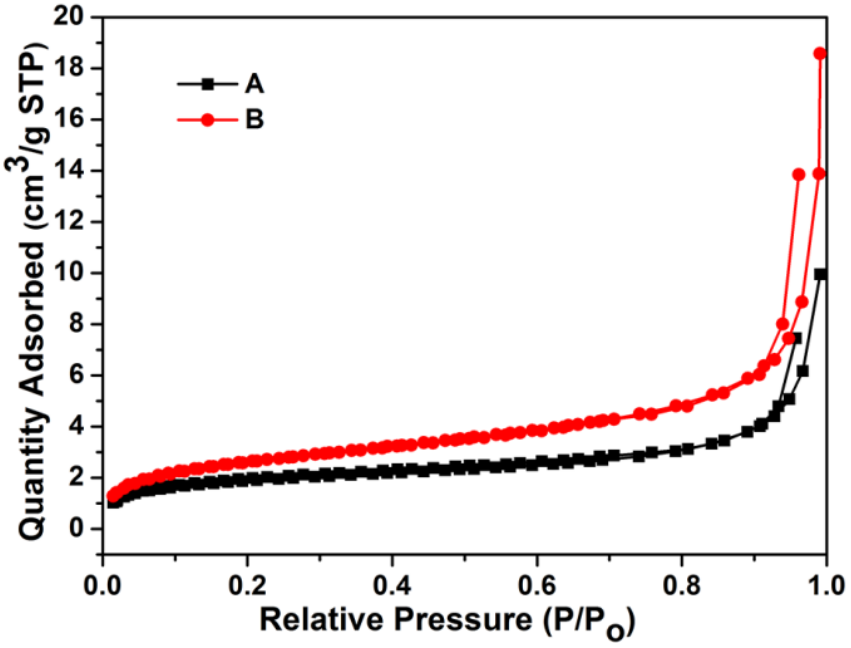

Figure S11 N_2 adsorption-desorption isotherms of Al-MOFs (A) and Fe_3O_4/RhB@Al-MOFs (B)

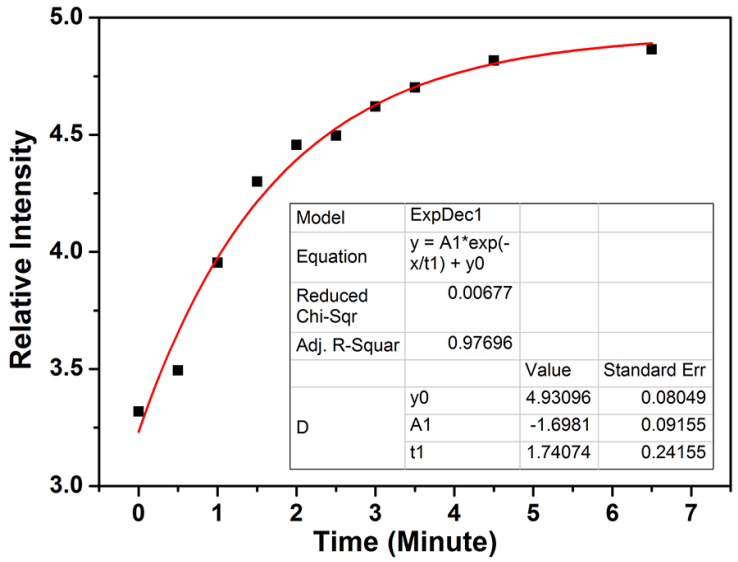

Figure S12 The kinetic study of the response of Fe_3O_4/RhB@Al-MOFs to Mg^{2+} ions (1 x 10^{-3}M) under pseudo-first-order conditions. Slope = -0.5745 min^{-1}

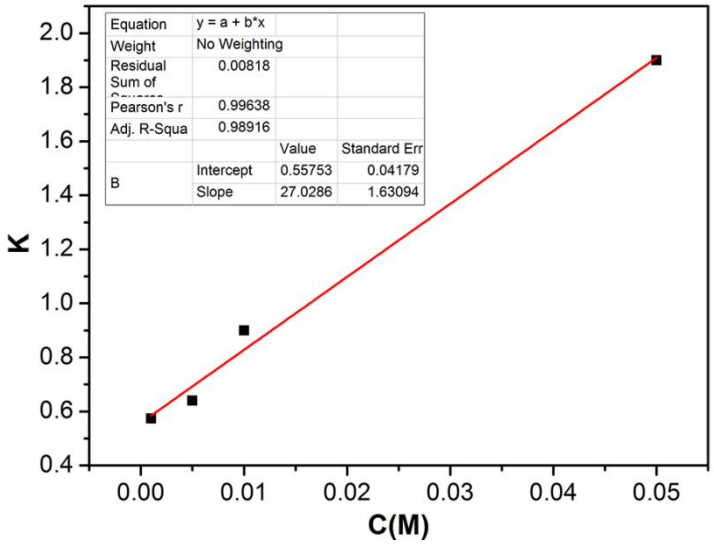

Figure S13 Plot of the observed k versus the concentration of Mg^{2+} ions for the pseudo first-order reaction of Fe_3O_4/RhB@Al-MOFs with varying concentration of Mg^{2+} Slope = 27.0286 $M^{-1}min^{-1}$

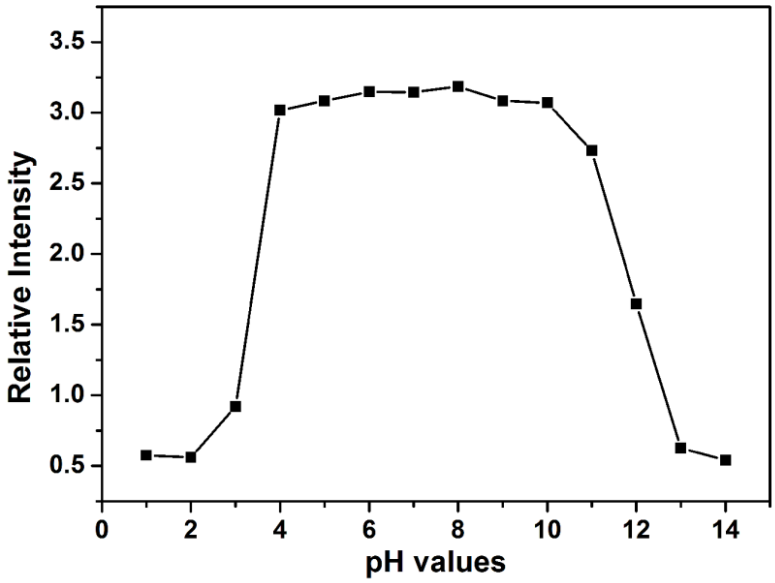

Figure S14 Fluorescence measurements of Fe_3O_4/RhB@Al-MOFs after treatment with different pH

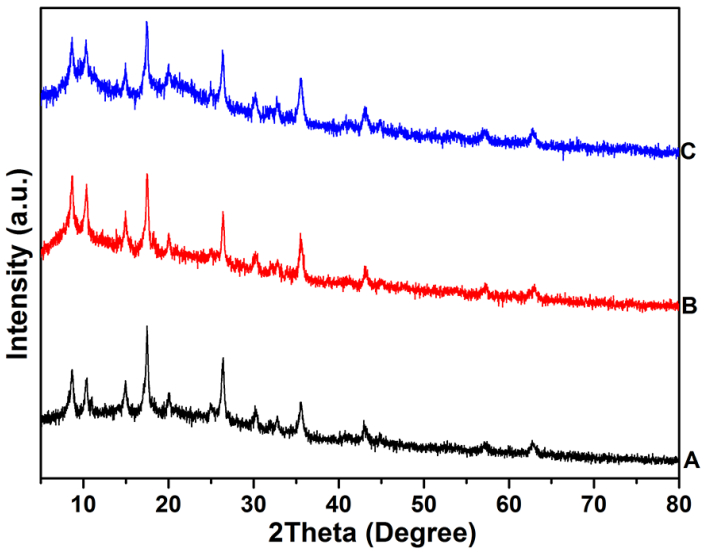

Figure S15 XRD patterns of as-synthesized Fe_3O_4/RhB@Al-MOFs (A), Fe_3O_4/RhB@Al-MOFs after detection of Mg^{2+} ions for five cycles (B) and Fe_3O_4/RhB@Al-MOFs after storaging in water for 7 days (C)

Table 1 Comparison table for various probes for the detection of Mg^{2+} ions.

Probe	Metal	Detect limit	Application	Ref
4-hydroxy-5-isopropyl-2 thylisophthalaldehyde	Mg^{2+}	2.70×10^{-6} M	Fluorescent "turn-on" sensor	[14]
4-hydroxy-3-((2-hydroxy-5-methylphenyl)diazenyl)-2Hchromen-2-one	Mg^{2+}	2.4×10^{-8} M	Fluorescent "turn-off" sensor	[15]
8-hydroxyquinoline-5-carbaldehyde-(benzotriazol-1 - acetyl)	Mg^{2+}	_	Fluorescent "turn-on" sensor	[16]
(Z)-2-hydroxy-N-(2-hydroxybenzylidene)benzohydrazide	Mg^{2+}	1.7×10^{-7} M	Fluorescent "turn-on" sensor	[17]
(E)-2-((2-(pyridin-2-l)hydrazono)methyl)quinolin-8-ol	Mg^{2+}	1.9×10^{-7} M	Fluorescent "turn-on" sensor	[18]
$\{[Ln(L)_3Fe_{1.5}(H_2O)_3]_{1.5}H_2O\}n$	Mg^{2+}	_	Fluorescent "turn-on" sensor	[19]
$[LnAg(PDA)_2(H_2O)_3]_3H_2O\}n$	Mg^{2+}	_	Fluorescent "turn-on" sensor	[20]
8-HQC-PTH	Mg^{2+}	4.7×10^{-8} M	Ratiomenic Fluorescent sensor	[21]
2-hydroxy-5-methyl-1,3-phenylene)bis(methanylylidene)bis(isoquinoline-1-carbohydrazide	Mg^{2+}	2.97×10^{-8} M	Fluorescent "turn-on" sensor Intracellular detetion; plant tissues detetion	[22]
Fe_3O_4/RhB@Al-MOFs	Mg^{2+}	8×10^{-7} M	Ratiomenic Fluorescent "turn-on"sensor; Intracellular detetion; Magnetic recycling	This work

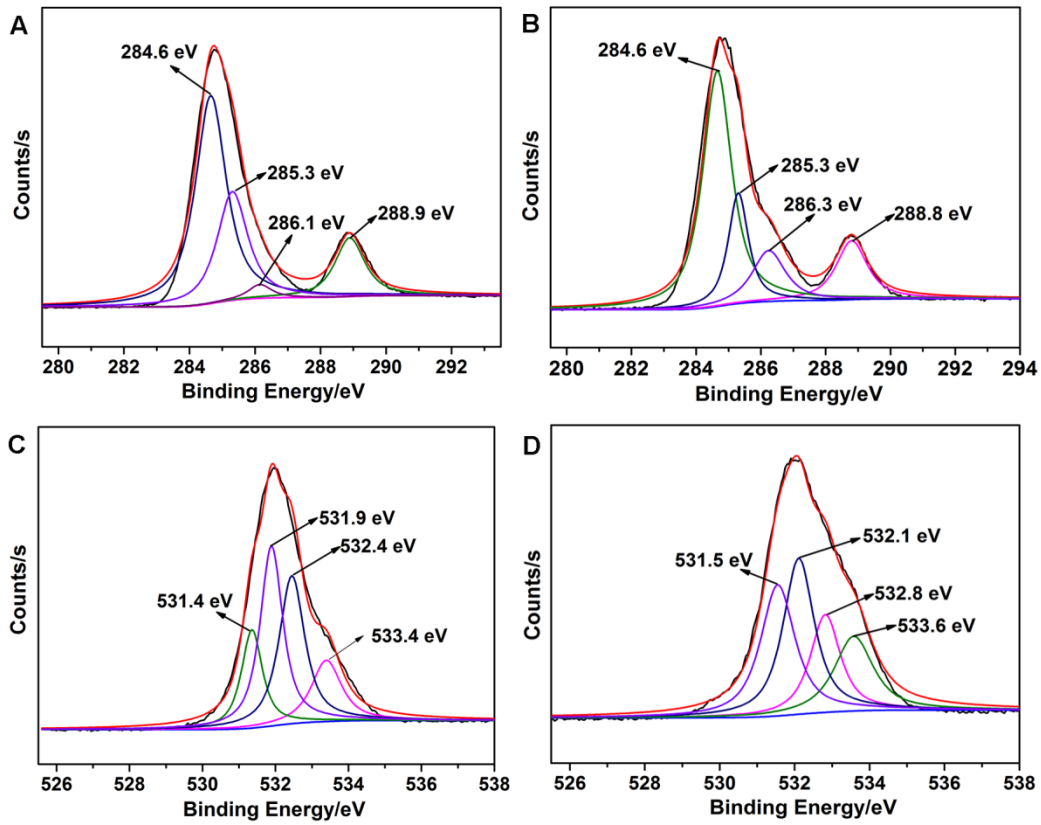

Figure S16 (A, B) C1s XPS for Fe_3O_4/RhB@Al-MOFs and Mg^{2+} treatment of Fe_3O_4/RhB@Al-MOFs; (C, D) O1s XPS for Fe_3O_4/RhB@Al-MOFs and Mg^{2+} treatment of Fe_3O_4/RhB@Al-MOFs

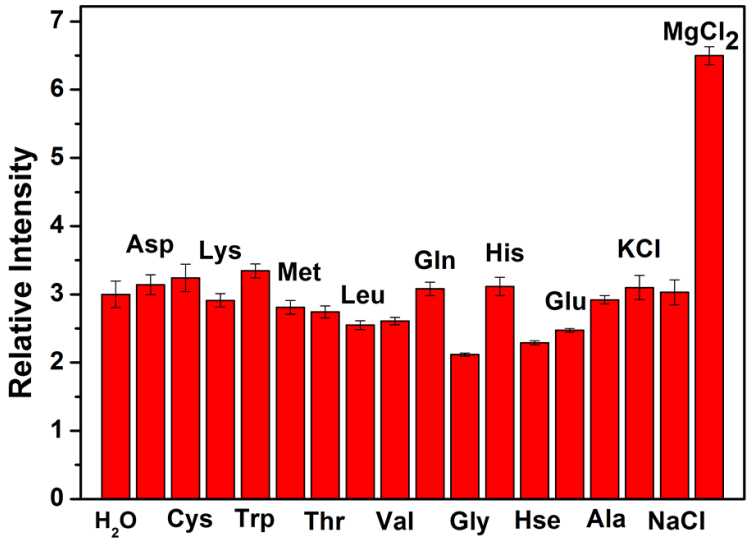

Figure S17 Comparison of the luminescence intensity of Fe_3O_4/RhB@Al-MOFs (I_{440}/I_{610}) in 10^{-3} M solutions of different biologically relevant substances

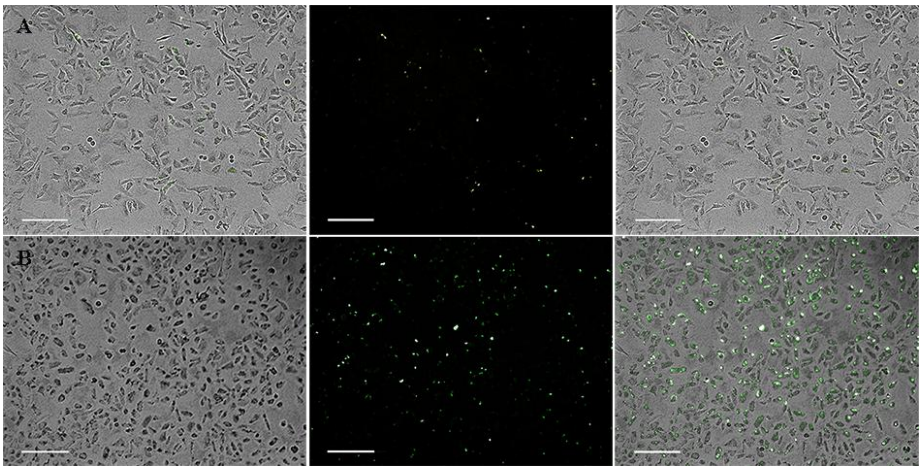

Figure S18 Fluorescence imaging of live A375 cells after being incubated with Fe_3O_4/RhB@Al-MOFs composite material (A); Fluorescence imaging of live A375 cells after being incubated with Fe_3O_4/RhB@Al-MOFs and Mg^{2+} ions (B). The left panels show dark-field fluorescence images, the middle panels show the corresponding bright-field images and the right panels are overlays of the left and middle panels. Scale bar: 200 μm.

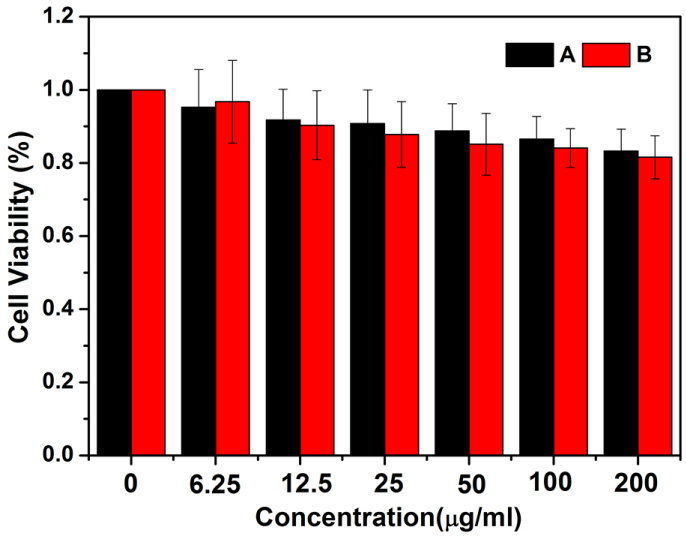

Figure S19 Viabilities of HL-7702 cells and A373 cells in the presence of Fe_3O_4/RhB@Al-MOFs composite assessed by MTT.